Inorganic Chemistry
Article
Cite This: Inorg. Chem. XXXX, XXX, XXX−XXX
pubs.acs.org/IC

One-Pot Catalytic Cleavage of C═S Double Bonds by Pd Catalysts at Room Temperature

Ting Zhu,[†,#] Xiaoxi Wu,[‡,#] Xinzheng Yang,[§,∥,#] Bigyan Sharma,[†] Na Li,[⊥] Jiaming Huang,[§] Wentao Wang,[§] Wang Xing,[†] Zhenwen Zhao,[⊥] and Hui Huang*[,†]

[†]College of Materials Science and Optoelectronic Technology & CAS Key Laboratory of Vacuum Physics, [‡]Sino-Danish College, and [§]College of Chemistry and Chemical Engineering, University of Chinese Academy of Sciences, Beijing 100049, PR China

[∥]State Key Laboratory for Structural Chemistry of Unstable and Stable Species, CAS Research/Education Center for Excellence in Molecular Sciences and [⊥]Key Laboratory of Analytical Chemistry for Living Biosystems, Beijing Mass Spectrum Center, Beijing National Laboratory for Molecular Sciences, Institute of Chemistry, Chinese Academy of Sciences, Beijing 100190, PR China

Supporting Information

ABSTRACT: The C═S double bonds in CS_2 and thioketones were catalytically cleaved by Pd dimeric complexes $[(N^{\wedge}N)_2Pd_2(NO_3)_2](NO_3)_2$ (N^N, 2,2′-bipyridine, 4,4′-dimethylbipyridine or 4,4′-bis(trifluoromethyl)) at room temperature in one pot to afford CO_2 and ketones, respectively, for the first time. The mechanisms were fully investigated by kinetic NMR, isotope-labeled experiments, in situ ESI-MS, and DFT calculations. The reaction is involved a hydrolytic desulfurization process to generate C═O double bonds and a trinuclear cluster, which plays a pivotal role in the catalytic cycle to regenerate the dimeric catalysts with HNO_3. Furthermore, the electronic properties of catalyst ligands possess significant influence on reaction rates and kinetic parameters. At the same temperature, the reaction rate is consistent with the order of electronegativity of N^N ligands (4,4′-bis(trifluoromethyl) > 2,2′-bipyridine > 4,4′-dimethylbipyridine). This homogeneous catalytic reaction features mild conditions, a broad substrate scope, and operational simplicity, affording insight into the mechanism of catalytic activation of carbon sulfur bonds.

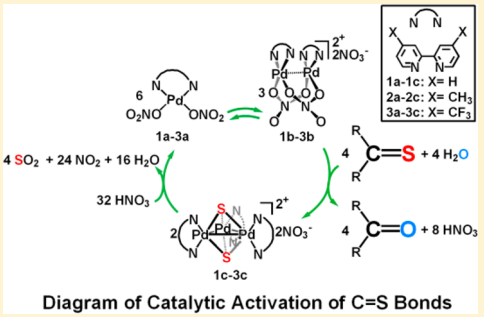

Diagram of Catalytic Activation of C=S Bonds

INTRODUCTION

Catalytic activation of carbon sulfur bond is important due to its wide applications in chemical,[1−3] energy,[4] and environmental industry.[5,6] Hydrodesulfurization (HDS), the conversion of organic sulfur compounds to hydrogen sulfide and hydrocarbons by catalytic technologies, is one of the most important steps in petroleum refining industry, since fossil fuel usually contain organic sulfur impurities.[6,7] Furthermore, conversion of hazardous sulfur compounds to harmless chemicals is critical for environmental protection. In general, industrial-scale sulfur removal is carried out through heterogeneous catalysis,[8,9] while the mechanisms are still under investigation.[10,11] Thus, many efforts have been dedicated to the carbon−sulfur bond activation with transition metal complexes to probe the mechanism for developing highly efficient industrial catalysts.[12,13] Different transition metals have been employed to mediate the C−S bond activation, including palladium,[14−16] platinum,[17,18] rhodium,[19−22] iridium,[23,24] copper,[25,26] nickel,[27,28] iron,[18,29] cobalt,[30,31] ruthenium,[32,33] tungsten,[34] and niobium,[35,36] among others.

Activation of C−S single bond has been realized in different systems, while activation of carbon−sulfur double bonds (C═S) is fundamentally interesting and extremely challenging since the C═S double bond, especially the second C−S bond, is very inert due to large bond dissociation enthalpy (171.5 kcal/mol for free CS).[37] Thus, the cleavage of both bonds in a C═S double bond is very rare[19] even though the first C═S bond activation has been well-documented.[12,41] For example, Nikonov et al. activated the stable C═S bond through oxidative addition of an Al[1] compound, resulting in an aluminum sulfide with a terminal Al═S bond, which was confirmed with single crystal X-ray diffraction and DFT calculations.[38] Also, Fryzuk and co-workers employed a ditantalum complex to fully cleave both C═S double bonds of CS_2 to generate a complex with two bridging sulfides and a bridging methylene unit, which was further treated with H_2 to produce CH_4 and a disulfide complex.[39] Furthermore, Laubenstein et al. used rhodium(I) complexes to successfully cleave the C═O double bonds of CO_2 and C═S double bond of CS_2 to afford a carbide complex.[40] However, none of these reactions was achieved with a catalytic cycle, which is the key step to commercialize the catalytic technologies.

The kinetic parameters of the cleavage of single C−S bonds have been widely studied theoretically and experimentally to probe the mechanisms.[42−46] Nevertheless, to the best of our knowledge, the activation enthalpy ($\Delta H^{\ddagger}$) and entropy values ($\Delta S^{\ddagger}$) have never been reported for C═S double bond activation. This may be due to the lack of successful systems

Received: May 10, 2018

DOI: 10.1021/acs.inorgchem.8b01275
Inorg. Chem. XXXX, XXX, XXX−XXX

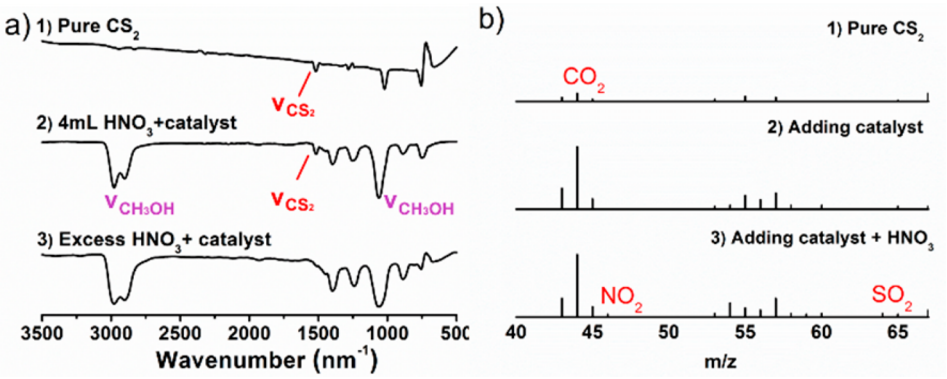

Figure 1. Fourier transform infrared spectroscopy (a) and gas chromatography mass spectrometry (b) for the one-pot reaction of CS_2 with HNO_3.

for C═S bond activation. Recently, we hydrolytically cleaved the C═S double bonds of CS_2 with dimeric Pd complexes at room temperature, of which mechanism was studied by DFT calculations. Furthermore, a "pseudo" catalytic cycle was achieved based on two independent reactions.[47] Thus, it is urgent to develop the methodology and deeply investigate the mechanism due to its great potential in different applications.

Herein, we developed a series of dimeric palladium complexes to successfully realized one-pot catalytic activation of C═S bonds in both inorganic and organic compounds for the first time. The catalytic mechanisms were systematically investigated with different techniques. The dynamic ^{1}H NMR studies showed that the electronic properties of ligands have strong effects on the kinetic parameters of C═S bond activation in CS_2 which supports the theoretical studies. Also, a trinuclear cluster plays a pivotal role in the catalytic cycle of activation of thioketone, which was supported by mercury experiments, isotope-labeling experiment, electrospray ionization mass spectrometry (ESI-MS), and DFT calculations.

RESULTS AND DISCUSSION

Dimeric Pd complexes $[(N^\wedge N)_2Pd_2(NO_3)_2](NO_3)_2$ (N^N, 2,2′-bipyridine or 4,4′-dimethylbipyridine) with different organic ligands were synthesized according to the reported method.[48,49] The structure of $[(N^\wedge N)_2Pd_2(NO_3)_2](NO_3)_2$ (N^N, 4,4′-bis(trifluoromethyl)) was confirmed by ^{1}HNMR and ESI-MS (Figures S8 and S9). ^{1}H NMR spectrum demonstrates three signals in the range of 8.0−9.2 ppm, corresponding to the three types of protons in the aromatic rings of **3b·2NO$_3$**. ESI-MS spectrum showed a mass-to-charge ratio (m/z) at 460.0, which supported the structure of **3b** in water being dimeric, similar to those of **1b** and **2b**. Furthermore, aqueous complex **3a·2NO$_3$** was treated with CS_2 to yield cluster **3c·2NO$_3$** and CO_2 upon cleavage of the C═S bonds. Thus, it is reasonably to conclude that **3b·2NO$_3$** may possess reactivity similar to those of **1b·2NO$_3$** and **2b·2NO$_3$**.

The dimeric Pd complex (**1b·2NO$_3$**) was dissolved in a mixture solvent of water and methanol (1:3). After addition of 10 equiv of CS_2, the solution stayed clear since the produced Pd−S cluster is soluble under this circumstance, which is different from the reported results that Pd-clusters precipitated in the aqueous solution.[47] Next, a methanol solution of HNO_3 was added dropwise to catalytically oxidize the CS_2 until its full conversion. In order to identify the products of the reaction, gas chromatography mass spectrometry (GC-MS) and Fourier transform infrared spectroscopy (FT-IR) were employed to monitor the reaction (Figure 1). In GC-MS, only the signal at m/z = 44 corresponding to the CO_2 in air was observed in the atmosphere of pure CS_2 (Figure 1b), which may be rooted from the GC-MS machine being under atmosphere. Upon addition of aqueous complex **1b·2NO$_3$**, the intensity of the signal at m/z 44 increased, indicating generation of CO_2 from the reaction. Furthermore, two new signals (m/z 46 and 64) were observed after addition of methanol solution of HNO_3, suggesting the generation of NO_2 and SO_2, respectively. In FT-IR spectra (Figure 1a), a broad peak at 1500 cm^{-1} corresponding to C−S stretching was observed in the methanol solution of CS_2. Upon addition of HNO_3, the peak continuously decreased until fully disappeared, which proved that the CS_2 was consumed. Therefore, a one-pot catalytic conversion of CS_2 with HNO_3 to CO_2 and SO_2 by dimeric Pd catalyst **1b·2NO$_3$** was successfully achieved under room temperature, which is an important progress to develop this methodology in comparison to the reported two-steps catalysis.[47]

In order to probe the mechanism of C═S bond activation, time-resolved ^{1}H NMR was used to monitor the appearance of the H_δ resonances of **1c·2NO$_3$** and H_α resonances of **2c·2NO$_3$** and **3c·2NO$_3$** throughout the whole reaction over the 298.15−313.15K range of temperature for investigating the influence of the electronic properties of ligands on kinetic parameters. The kinetic control (25 °C, sealed NMR tube) experiment shows that reaction of CS_2 with complex **1b·2NO$_3$** leads to the formation of complex **1c·2NO$_3$** (Figure 2). As the kinetic investigations were performed in the presence of a large excess of CS_2 (>30 equiv) and D_2O (>100 equiv), the whole rate law is reasonably taken as for a pseudo-first-order reaction:

$$v = -\frac{\mathrm{d}[\mathbf{1a}]}{\mathrm{d}t} = k[\mathbf{1a}][CS_2][H_2O] = k_{obs}[\mathbf{1a}] \quad (1)$$

Under such conditions the reaction as shown in Scheme 1 went to completion. The values of rate constant at different temperatures (k in M^{-1} s^{-1}) were obtained by dividing pseudo-first-order rate constants (k_{obs} in s^{-1}) by the concentration of CS_2 and H_2O, which are reported in Table 1. To complete the analysis and reduce errors, the activation parameters are determined by Arrhenius plot and Eyring plot methods.

Not surprisingly, the rate constant improved when temperature increased, which is consistent with the law that the rate increases 2−4 times when the temperature increased by 10 °C based on Arrhenius equation.[50] Also, at the same temperature, the reaction rate is consistent with the order of electronegativity of ligands ((X = CF_3) > (X = H) > X = (CH_3))

DOI: 10.1021/acs.inorgchem.8b01275
Inorg. Chem. XXXX, XXX, XXX−XXX

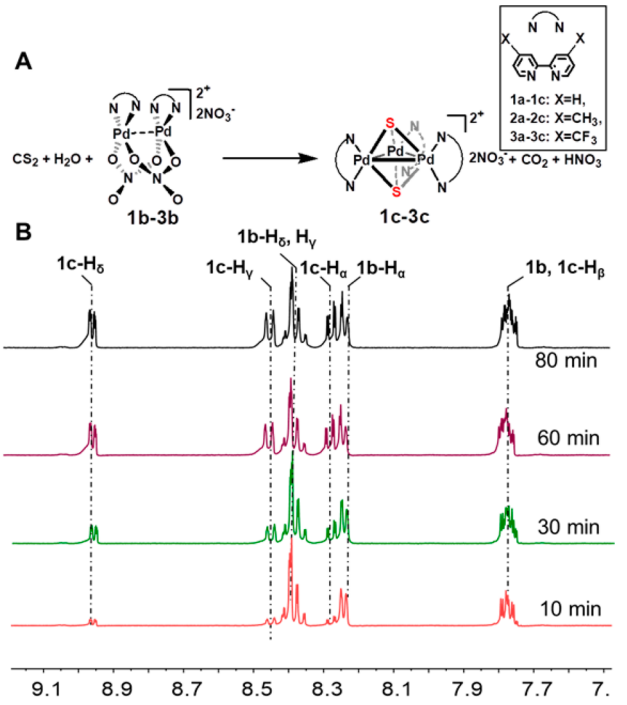

Figure 2. (A) Reaction of CS_2 with aqueous complex **1b·2NO$_3$**−**3b·2NO$_3$**. (B) Representative ^{1}H NMR spectroscopy of monitoring the reaction of **1b·2NO$_3$** and CS_2 (25 °C in methanol-d_4, sealed NMR tube).

Scheme 1. Schematic Diagram of Mechanism of the Catalytic Reaction

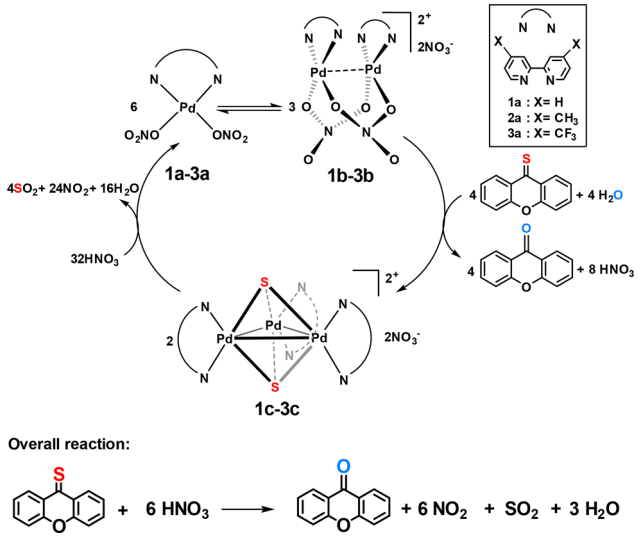

(Table 1, entries 1−12). According to a $\Delta\Delta G^{\ddagger}$ value at the same temperature, the reaction rate of CS_2 with **3b·2NO$_3$** is 1.3−1.8 times faster than that with **1b·2NO$_3$**, which is 3−4 times faster than that with **2b·2NO$_3$**. The Eyring analysis of k values as a function of temperature provides more details[47] (Figure 3). (1) The reduction of rate constant is mainly because of the increase in $\Delta H^{\ddagger}$ ($\Delta\Delta H^{\ddagger}$ = 28.7 kJ mol^{-1}) for **1b·2NO$_3$** and **2b·2NO$_3$**. (2) According to the associative nature of the reaction, $\Delta S^{\ddagger}$ is negative, but the absolute value of **1b·2NO$_3$** is higher in the case of **3b·2NO$_3$** by about 50 J mol^{-1}, which causes the difference of k values. Previous DFT study shows that the rate-determining step in the cleavage of C−S bond is associated with **13** to **TS4** (Figure S16).[47] Obviously, the electron-donating ligand (X = CH_3) leads to an increase of the activation barrier, while electron-withdrawing ligand (X = CF_3) stabilizes the negative charge build-up in the transition state, thereby lowering the energy barrier of the rate-determining step of **13** to **T4** (Figure S16).[42−46] Thus, the kinetic studies are consistent with the theoretical results.[47] This is likely attribute to (1) the introduction of polar groups in γ-position of aromatic ring could compensate the loss of entropy[51] and (2) the build-up of negative charge or the decrease of positive charge in the γ-position of aromatic ring in the rate-determining transition state.[52]

To prove the versatility of C═S bonds catalytic activation for both organic and inorganic sulfide compounds and promote the methods of sulfur removal for environmental protection, this methodology was developed for converting thioketones, which are important chemicals for organic sulfur synthetic chemistry,[53] pharmaceutical,[54] and electronic applications.[55] As shown in Table 2, thioketones **4a**−**8a** were treated with nitric acid in the presence of 10 mol % **1a·2NO$_3$** to generate corresponding ketones **4b**−**8b** with yields of 70−93%, together with NO_2 and SO_2. Note that under the same conditions the conversion of thioketone **9a** to ketone **9b** was only 5.6%. A mixed solvent of H_2O/THF (3:2) was chosen to ensure the homogeneous conditions. The produced ketones were confirmed with ^{1}H and ^{13}C NMR, elementary analysis, while the NO_2 and SO_2 were identified with GC-MS with signals at m/z 46 and 64, respectively (Figures S23−S35). To test the efficacy of the catalyst, a small loading (1% mol) of the catalyst was used to convert the thioketones (entry 2). Interesting, ketones were also achieved with a high yield of 90%, which showed the high efficiency of this catalyst. Two other dimeric Pd complexes (**2b·2NO$_3$**−**3b·2NO$_3$**) were employed as catalysts to cleave the C═S bonds of thioketone **4a** to demonstrate the catalytic versatility of the dimeric Pd complexes. Not surprisingly, both complexes catalytically converted thioketone **4a** to ketone **4b** with nitric acid as the oxidant with high yields of 80−90%. Furthermore, treatment of these two Pd complexes with THF solution of **4a** yielded **4b** and the corresponding trinuclear Pd clusters (**2c·2NO$_3$** and **3c·2NO$_3$**). According to the turnover number (TON) and turnover frequency (TOF), the **3b·2NO$_3$** demonstrated the highest catalytic efficiency (Table S1). These results indicate that the dimeric Pd cores of the catalyst played an important role in the catalytic cycles.

A negative mercury-drop assay suggested that the catalytic reaction is homogeneous and Pd nanoparticles play no role in the C═S bonds cleavage process. Furthermore, the control reaction that treatment of aqueous solution of **4a** with HNO_3 (dilute or concentrated) at room temperature does not produce detectable amounts of ketone, NO_2, and SO_2 at room temperature, which supported the pivotal role of the dimeric Pd catalysts in this process.

To investigate the mechanisms of the catalytic reactions, a THF solution of **4a** was chosen as an example to be treated with aqueous solution of **1a·2NO$_3$** to yield **4b**, trinuclear $[(N\hat{}N)_3Pd_3(\mu_3\text{-}S)_2](NO_3)_2$ cluster (**1c·2NO$_3$**), and HNO_3 at room temperature in several minutes. The generation of **1c** cluster was confirmed by ^{1}H NMR and ESI-MS, which is the same as the reported results.[47] Furthermore, the pH values of the solution initially dropped followed by obvious increase as shown in Figure S37. This indicates that H^+ was generated first followed by slowly reacting with the cluster to regenerate the

DOI: 10.1021/acs.inorgchem.8b01275
Inorg. Chem. XXXX, XXX, XXX−XXX

Table 1. Rate Constant k (M^{-1} s^{-1}) as a Function of Temperature T (K) and Activation Parameters $\Delta H^{\ddagger}$ (kJ/mol), $\Delta S^{\ddagger}$ (J/mol), and $\Delta G^{\ddagger}$ (kJ/mol) for the Reaction Shown in Figure 2a

entry	T (K)	$k \times 10^8$	$\Delta G^{\ddagger}$	$\Delta H^{\ddagger}$	$\Delta S^{\ddagger}$
			X = CH_3		
1	298.15	1.98 ± 0.10	115.8 ± 12.6	103.4 ± 6.4	−41 ± 21
2	303.15	3.84 ± 0.04	116.0 ± 12.6		
3	308.15	6.91 ± 0.58	116.2 ± 12.8		
4	313.15	15.9 ± 0.88	116.4 ± 12.9		
			X = H		
5	298.15	8.99 ± 0.12	113.3 ± 6.5	74.7 ± 3.3	−130 ± 11
6	303.15	14.15 ± 0.44	114.0 ± 6.6		
7	308.15	23.04 ± 0.45	115.0 ± 6.6		
8	313.15	40.13 ± 0.89	115.0 ± 6.7		
			X = CF_3		
9	298.15	12.16 ± 0.10	112.6 ± 5.7	91.7 ± 2.9	−70 ± 9
10	303.15	21.04 ± 0.38	112.9 ± 5.7		
11	308.15	40.45 ± 0.67	113.3 ± 5.8		
12	313.15	74.03 ± 1.36	113.6 ± 5.8		

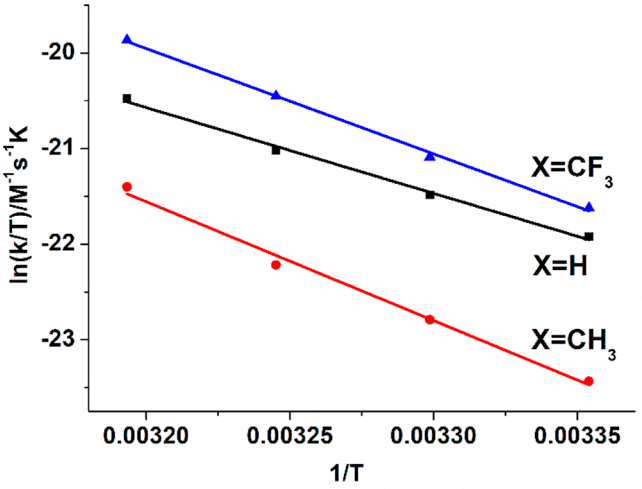

Figure 3. Eyring plots for the cleavage of C−S bonds in CS_2 by three different catalysts in methanol-d_4.

catalyst. To identify the role of H_2O in the reaction, a THF solution of **4a** was treated with a THF solution of **1a·2NO$_3$** at room temperature. Not surprisingly, no reaction was observed, indicating the essential role of H_2O. To further identify the sources of the oxygen in ketone, an isotope-labeled experiment was carried out with $H_2{}^{18}O$. Interestingly, when **4a** was treated with **1a·2NO$_3$** in $H_2{}^{18}O$ solution, the isolated ketone afforded a molecular ion at m/z 198 corresponding to ^{18}O-labled **4b**, which suggests the oxygen atom in ketone originates from the H_2O (Figure S38).

Moreover, treatment of trinuclear cluster **1c·2NO$_3$** with nitric acid regenerated dimeric Pd complexes **1b·2NO$_3$**, together with SO_2 and NO_2, the same as the reported results.[47] These two steps successfully achieved a catalytic cycle of thioketone reacting with HNO_3, which revealed that the trinuclear cluster may be a critical intermediate to achieve the catalytic cycle. Also, a THF solution of **9a** was treated with an aqueous solution of **1a·2NO$_3$** to afford **9b** and a mixed of unidentified palladium complexes. Not surprisingly, treatment of these unidentified palladium complexes does not regenerate the dimeric Pd complex, **1b·2NO$_3$**. This observation may explain the extremely low yield (5.6%) of the reaction of thioketone with HNO_3 in the presence of catalytic amount of

Table 2. Catalytic Activation of C═S Bonds of Thioketones by One-Pot Reaction

Entry	Substrate	Product	Catalyst loading (%)	Time (h)	Yield (%)	TON	TOF(10^{-3} s^{-1})
1	 4a	 4b	10	2	93	9.3	1.29
2	 4a	 4b	1	2	90	9	1.25
3	 5a	 5b	10	2	91	9.1	1.26
4	 6a	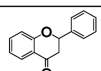 6b	10	3	89	8.9	0.82
5	 7a	 7b	10	2	85	8.5	1.18
6	 8a	 8b	10	3	70	7.0	0.65
7	 9a	 9b	10	3	5.6	0.56	0.08

1a·2NO$_3$, supporting the key role of the cluster $[(N\hat{}N)_3Pd_3(\mu_3\text{-}S)_2](NO_3)_2$ as the intermediate in the catalytic cycle. Thus, a catalytic cycle was proposed as shown in Scheme 1. Thioketones reacted with the dimeric Pd complex through hydrolysis to generate ketone, trinuclear Pd cluster, and nitric acid. Next, the trinuclear Pd cluster reacted with nitric acid to regenerate the dimeric Pd complex, together with SO_2 and NO_2.

To further reveal the mechanism of the reaction between dimeric Pd and thioketone, on-line ESI-MS was employed to monitor the reaction of **4a** with the dimeric Pd complex **1b·**

DOI: 10.1021/acs.inorgchem.8b01275
Inorg. Chem. XXXX, XXX, XXX−XXX

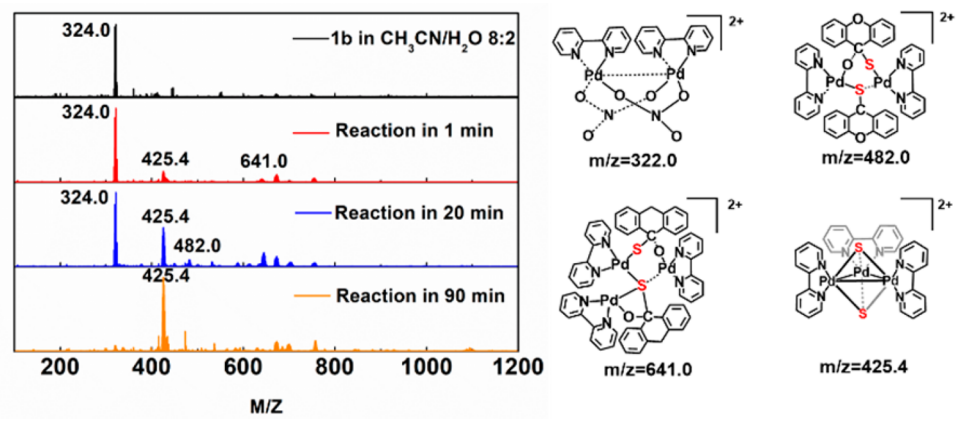

Figure 4. Monitoring the reaction of thioketone **4a** with aqueous of **1a** by on-line ESI−MS at a function of time. The signals at m/z 324.0 and 425.4 correspond to $[\mathbf{1b}\cdot\mathbf{NO_3}]^+$ and $[\mathbf{1c}]^{2+}$, respectively. t = 0, 1, 20, and 90 min.

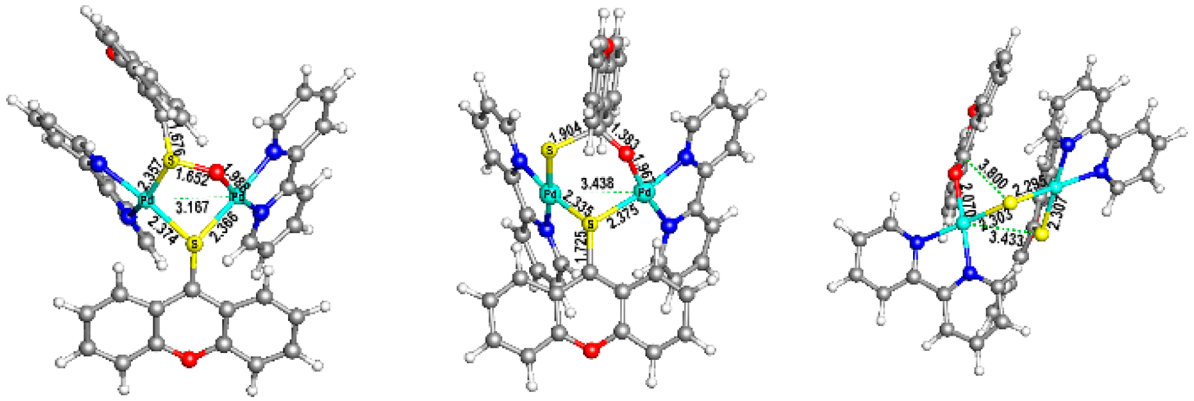

Figure 5. Three optimized isomer structures of m/z = 482.0.

$\mathbf{2NO_3}$. ESI-MS before the addition of **4a** revealed an ion at m/z 324.0, corresponding to complex $[\mathbf{1b}\cdot\mathbf{NO_3}]^+$. Upon addition of **4a**, low-intensity features at m/z 482.0 and 641.0 were observed and assigned to fragmentation ion $\{[(bpy)Pd]_2[(C_6H_4)_2(O)(C)]_2(\mu\text{-}O)(\mu\text{-}S)_2\}^{2+}$ and $\{[(bpy)Pd]_3[(C_6H_4)_2(O)(C)]_2(\mu\text{-}O)_2(\mu\text{-}S)_2\}^{2+}$, respectively, as proposed based on classic coordination chemistry. After 90 min, these signals disappeared, while the signal of final product $[\mathbf{1c}]^{2+}$ appeared at m/z 425.4 (Figure 4).

Density functional theory (DFT) calculations were performed to exam the structures of some key intermediates which were observed in the ESI-MS spectra. Computational details and relative energies of those structures are listed in the Supporting Information. The optimized structures of **1b** and **1c** are shown in Figure S41. Complex **1c** possesses a D_{3h} symmetry with two sulfur atoms at the center of the molecular, consistent with the reported crystal structure.[42−46] The optimized structures of three isomers for the intermediate of m/z = 482.0 are shown in Figure 5. We can observe the breaking of C═S bond and the formation of C═O bond in those three structures. Interestingly, the structure with a newly formed ketone molecule bonding to Pd (**482-3**) is the most stable one. Three structures for m/z = 641.0 (Figure S42) were also computationally predicted, and we found that the **1c** with two noncovalent bonding ketone molecules (**641−3**) is the most stable one. These results elucidate the presence of the intermediates observed in on-line ESI-MS.

CONCLUSIONS

In conclusion, dimeric Pd complexes were employed to catalytically cleave the C═S bonds of CS_2 and thioketones in one pot for the first time. The mechanism on C═S bond activation of CS_2 was probed by dynamic ^{1}H NMR to investigate the influence of electronic properties of ligands on the kinetic parameters, which supports the theoretical results. Furthermore, the catalytic mechanism of thioketones activation was investigated by isotope-labeling experiment, on-line ESI-MS, and DFT calculations, which showed that the trinuclear clusters play important roles as intermediates for the catalysis. This contribution paved a new route for catalytic activation of carbon−sulfur bond and shed lights on understanding the mechanism.

EXPERIMENTAL SECTION

Materials and General Methods. All reactions were carried out in flame-dried glassware under an atmosphere of dry N_2 with the exclusion of air and moisture using standard Schlenk techniques. All organic solvents were freshly distilled from sodium benzophenone ketyl immediately prior to use air- and moisture-sensitive liquids and solutions were transferred by syringe. Reactions were stirred using Teflon-coated magnetic stir bars. Elevated temperatures were maintained using Thermostat-controlled silicone oil baths. Organic solutions were concentrated using a rotary evaporator with a diaphragm vacuum pump. Analytical TLC was performed on silica gel GF254 plates. The TLC plates were visualized by ultraviolet light (λ = 254 nm). Purification of products was accomplished by flash

DOI: 10.1021/acs.inorgchem.8b01275
Inorg. Chem. XXXX, XXX, XXX−XXX

column chromatography on silica gel (Innochem SilicaFlashP60, 200−300 mesh). Other chemicals were purchased from various commercial sources and were used as received. Substrates 9*H*-xanthene-9-thione, di-2-thienylmethanethione, 4-flavanthione, 9*H*-fluorene-9-thione, 4*H*-1-benzopyran-4-thione, and 7*H*-benz[*de*]-anthracene-7-thione were synthesized following the published procedures. NMR spectra were recorded on a JNM-ECZ 400 MHz nuclear magnetic resonance spectrometer. The ^{1}H NMR spectra were calibrated against the peak of tetramethylsilane (TMS, 0 ppm). GC analysis was performed on a Shimadzu GC-2010 instrument equipped with a FID detector using nitrogen as the carrier gas. ESI-FTIR mass spectrometric analysis was performed with a Bruker solariX mass spectrometer equipped with a 9.4 T superconducting magnet and SmartBeam laser optics.

Synthesis of 3b·2NO$_3$. A 100 mL flask was charged with bpy(CF$_3$)$_2$PdCl$_2$ (320 mg, 0.68 mmol)was suspended in 60 mL of dilute nitric acid (pH = 1) under N$_2$. A small amount of a water solution of AgNO$_3$ (232 mg, 1.36 mmol) was added dropwise into the tube. The mixture was stirred for 10 h at 60 °C under dark. After filtration, the solvent was removed to afford a yellow solid. Yield, 294 mg, 83%. ^{1}H NMR (400 MHz, methanol-d_4, 25 °C) δ = 8.96 (d, J = 2.0 Hz, 2H), 8.58 (d, J = 2.0 Hz, 2H), 8.20 (d, J = 0.8 Hz, 2H). ESI-MS Calcd for $C_{24}H_{12}F_{12}N_6O_6Pd_2^{2+}$: 459.9; found: 460.0.

■ ASSOCIATED CONTENT

Supporting Information

The Supporting Information is available free of charge on the ACS Publications website at DOI: 10.1021/acs.inorgchem.8b01275.

Synthesis and characterization details, reaction of CS_2 with **3b·2NO$_3$** and H_2O, FT-IR and GC-MS monitoring results, VT-NMR spectra, catalytic experiment of cleaving C═S bonds of thioketoes, mechanistic study, reaction of catalyst with thioketone, experimental details for monitoring pH during reaction of **4a** with **1b·2NO$_3$**, reaction of control without water, isotopic labeling methods, reaction of **4a** with **2b·2NO$_3$** and **3b·2NO$_3$**, on-line ESI-MS monitoring results, free energy and atomic coordinates of calculated structures (PDF)

■ AUTHOR INFORMATION

Corresponding Author

*E-mail: huihuang@ucas.ac.cn.

ORCID

Xinzheng Yang: 0000-0002-2036-1220
Zhenwen Zhao: 0000-0001-6127-808X
Hui Huang: 0000-0002-6102-2815

Author Contributions

#T.Z., X.W., and X.Y. contributed equally to this work.

Notes

The authors declare no competing financial interest.

■ ACKNOWLEDGMENTS

This work was supported by the NSFC (21774130 and 21574135), Beijing Natural Science Foundation (2162043), the Key Research Program of the Chinese Academy of Sciences (Grant No. XDPB08-2), One Hundred Talents Program of Chinese Academy of Sciences, and University of Chinese Academy of Sciences. DFT results described in this paper are obtained on the China Scientific Computing Gird (SCGrid).

■ REFERENCES

(1) Wang, M.; Fu, C.; Ma, S. Cleavage of oxygen−sulfur double bonds and carbon−sulfur bonds: unusual highly selective electrophilic addition of allenylic sulfoxides. *Chem. Sci.* **2013**, *4*, 1016−1022.

(2) Chung, M.-K.; Schlaf, M. A Catalytic Synthesis of Thiosilanes and Silthianes: Palladium Nanoparticle-Mediated Cross-Coupling of Silanes with Thio Phenyl and Thio Vinyl Ethers through Selective Carbon-Sulfur Bond Activation. *J. Am. Chem. Soc.* **2004**, *126*, 7386−7392.

(3) Neurock, M.; van Santen, R. A. Theory of Carbon-Sulfur Bond Activation by Small Metal Sulfide Particles. *J. Am. Chem. Soc.* **1994**, *116*, 4427−4439.

(4) Toutov, A. A.; Salata, M.; Fedorov, A.; Yang, Y.-F.; Liang, Y.; Cariou, R.; Betz, K. N.; Couzijn, E. P. A.; Shabaker, J. W.; Houk, K. N.; Grubbs, R. H. A potassium tert-butoxide and hydrosilane system for ultra-deep desulfurization of fuels. *Nature Energy* **2017**, *2*, 17008−17014.

(5) Ensafi, A. A.; Mansour, H. R.; Majlesi, R. Determination of trace amount of carbon disulfide in water by the spectrophotometric reaction-rate method. *Anal. Sci.* **2003**, *19*, 1679−1681.

(6) White, C. M.; Siriwardane, R. V.; Bockrath, B. C.; Hoffman, J. S.; Pennline, H. W.; Baltrus, J. The Sulfur Problem: Cleaning up Industrial Feed-stocks By Diane Stirling. Royal Society of Chemistry: London; 2001. 93 pp. *Energy Fuels* **2002**, *16*, 529.

(7) Ho, T. C. Deep HDS of diesel fuel: chemistry and catalysis. *Catal. Today* **2004**, *98*, 3−18.

(8) Javadli, R.; de Klerk, A. Desulfurization of heavy oil. *Appl. Petrochem. Res.* **2012**, *1*, 3−19.

(9) Korkmaz, S.; Salt, Y.; Hasanoglu, A.; Ozkan, S.; Salt, I.; Dincer, S. Pervaporation membrane reactor study for the esterification of acetic acid and isobutanol using polydimethylsiloxane membrane. *Appl. Catal. A: Gen.* **2009**, *366*, 102−107.

(10) Sushkevich, V. L.; Popov, A. G.; Ivanova, I. I. Sulfur-33 Isotope Tracing of the Hydrodesulfurization Process: Insights into the Reaction Mechanism, Catalyst Characterization and Improvement. *Angew. Chem., Int. Ed.* **2017**, *56*, 10872−10876.

(11) Prins, R.; Egorova, M.; Röthlisberger, A.; Zhao, Y.; Sivasankar, N.; Kukula, P. Mechanisms of hydrodesulfurization and hydrodenitrogenation. *Catal. Today* **2006**, *111*, 84−93.

(12) Wang, L.; He, W.; Yu, Z. Transition-metal mediated carbon-sulfur bond activation and transformations. *Chem. Soc. Rev.* **2013**, *42*, 599−621.

(13) Pan, F.; Shi, Z.-J. Recent Advances in Transition-Metal-Catalyzed C-S Activation: From Thioester to (Hetero)aryl Thioether. *ACS Catal.* **2014**, *4*, 280−288.

(14) Munjanja, L.; Brennessel, W. W.; Jones, W. D. Room-Temperature Carbon-Sulfur Bond Activation by a Reactive (dippe)Pd Fragment. *Organometallics* **2015**, *34*, 1716−1724.

(15) Chang, J.; Liu, B.; Yang, Y.; Wang, M. Pd-Catalyzed C-S Activation/Isocyanide Insertion/Hydrogenation Enables a Selective Aerobic Oxidation/Cyclization. *Org. Lett.* **2016**, *18*, 3984−3987.

(16) Blanchard, S.; Fensterbank, L.; Gontard, G.; Lacote, E.; Maestri, G.; Malacria, M. Synthesis of Triangular Tripalladium Cations as Noble-Metal Analogues of the Cyclopropenyl Cation. *Angew. Chem., Int. Ed.* **2014**, *53*, 1987−1991.

(17) Kundu, S.; Brennessel, W. W.; Jones, W. D. C-S Bond Activation of Thioesters Using Platinum(0). *Organometallics* **2011**, *30*, 5147−5154.

(18) Tan, R.; Song, D. C-H and C-S Activations of Quinoline-Functionalized Thiophenes by Platinum Complexes. *Organometallics* **2011**, *30*, 1637−1645.

(19) Zamostna, L.; Braun, T.; Braun, B. S-F and S-C Activation of SF_6 and SF_5 Derivatives at Rhodium: Conversion of SF_6 into H_2S. *Angew. Chem., Int. Ed.* **2014**, *53*, 2745−2749.

(20) Ren, P.; Pike, S. D.; Pernik, I.; Weller, A. S.; Willis, M. C. Rh-POP Pincer Xantphos Complexes for C-S and C-H Activation. Implications for Carbothiolation Catalysis. *Organometallics* **2015**, *34*, 711−723.

DOI: 10.1021/acs.inorgchem.8b01275
Inorg. Chem. XXXX, XXX, XXX−XXX

(21) Uetake, Y.; Niwa, T.; Hosoya, T. Rhodium-catalyzed ipso-borylation of alkylthioarenes via C-S bond cleavage. *Org. Lett.* **2016**, *18*, 2758−2761.
(22) Pan, F.; Wang, H.; Shen, P.-X.; Zhao, J.; Shi, Z.-J. Cross coupling of thioethers with aryl boroxines to construct biaryls via Rh catalyzed C-S activation. *Chem. Sci.* **2013**, *4*, 1573−1577.
(23) Das, U.; Ghorui, T.; Adhikari, B.; Roy, S.; Pramanik, S.; Pramanik, K. Iridium-mediated C-S bond activation and transformation: organoiridium(III) thioether, thiolato, sulfinato and thiyl radical compounds. Synthesis, mechanistic, spectral, electrochemical and theoretical aspects. *Dalton Trans.* **2015**, *44*, 8625−8639.
(24) Bianchini, C.; Casares, J. A.; Masi, D.; Meli, A.; Pohl, W.; Vizza, F. Insertion of iridium into C-H and C-S bonds of 2,5-dimethylthiophene, 2-methylbenzothiophene and 4,6-dimethyldibenzothiophene. *J. Organomet. Chem.* **1997**, *541*, 143−155.
(25) Rokob, T. A.; Rulisek, L.; Srogl, J.; Revesz, A.; Zins, E. L.; Schroder, D. On the Mechanism of the Copper-Mediated C-S Bond Formation in the Intramolecular Disproportionation of Imine Disulfides. *Inorg. Chem.* **2011**, *50*, 9968−9979.
(26) Diwan, K.; Singh, B.; Singh, S. K.; Drew, M. G. B.; Singh, N. Facile in situ copper(II) mediated C-S bond activation transforming dithiocarbamate to carbamate and thiocarbamate generating Cu(II) and Cu(I) complexes. *Dalton Trans.* **2012**, *41*, 367−369.
(27) Grochowski, M. R.; Li, T.; Brennessel, W. W.; Jones, W. D. Competitive Carbon-Sulfur vs Carbon-Carbon Bond Activation of 2-Cyanothiophene with $[Ni(dippe)H]_2$. *J. Am. Chem. Soc.* **2010**, *132*, 12412−12421.
(28) Wong, K.-T.; Yuan, T.-M.; Wang, M. C.; Tung, H.-H.; Luh, T.-Y. Chelation Assistance in the Activation of Csp^3-S Bonds in Nickel-Catalyzed Cross-Coupling Reactions. *J. Am. Chem. Soc.* **1994**, *116*, 8920−8929.
(29) Ortega-Alfaro, M. C.; Alcantara, O.; Orrala, M.; Lopez-Cortes, J. G.; Toscano, R. A.; Alvarez-Toledano, C. C-S bond activation of two novel asymmetric α-azo-ketenedithioacetals using $Fe_2(CO)_9$. *Organometallics* **2007**, *26*, 1895−1899.
(30) O'Connor, J. M.; Bunker, K. D.; Rheingold, A. L.; Zakharov, L. Sulfoxide Carbon-Sulfur Bond Activation. *J. Am. Chem. Soc.* **2005**, *127*, 4180−4181.
(31) Santra, B. K.; Lahiri, G. K. Ruthenium-, osmium- and cobalt-ion mediated selective activation of a C-Cl bond. Direct and spontaneous aromatic thiolation reaction via C-S bond cleavage. *J. Chem. Soc., Dalton Trans.* **1998**, *0*, 1613−1618.
(32) Alvarez-Toledano, C.; Delgado, E.; Donnadieu, B.; Gomez, M. A.; Hernandez, E.; Martin, G.; Ortega-Jimenez, F.; Zamora, F. Activation of C-S bonds in organosulfur compounds containing α,β-unsaturated ketone systems by carbonylruthenium and -iron complexes. *Eur. J. Inorg. Chem.* **2003**, *2003*, 562−568.
(33) Cabeza, J. A.; del Rio, I.; Garcia-Granda, S.; Riera, V.; Sanchez-Vega, M. G. Facile C-S bond activation of levamisole hydrochloride on a triruthenium cluster core. *Eur. J. Inorg. Chem.* **2002**, *2002*, 2561−2564.
(34) Mills, R. C.; Abboud, K. A.; Boncella, J. M. Carbon-sulfur bond activation of thiophenes by $[W(NPh)\{o\text{-}(Me_3SiN)_2C_6H_4\}(pyridine)_2]$. *Chem. Commun.* **2001**, *0*, 1506−1507.
(35) Coucouvanis, D.; Al-Ahmad, S.; Kim, C. G.; Koo, S. M. Activation and cleavage of the carbon-sulfur bond in niobium tert-butanethiolato complexes. Syntheses and structural characterizations of the tetrahedral and trigonal bipyramidal $[Ph_4P][NbV(S)_2(tert\text{-}BuS)_2]$ and $[Et_4N][NbV(S)(tert\text{-}BuS)_4]$ complexes. *Inorg. Chem.* **1992**, *31*, 2996−2998.
(36) Azevedo, N. P.; Lopes, A. R. G.; Silva, R. M.; Speziali, N. L.; Abras, A.; Horner, M.; Burrow, R. A. Formation of sulfido niobium complexes through C-S bond activation. *J. Braz. Chem. Soc.* **1998**, *9*, 279−285.
(37) Ariafard, A.; Brookes, N. J.; Stranger, R.; Yates, B. F. Activation of CS_2 and CS by ML_3 Complexes. *J. Am. Chem. Soc.* **2008**, *130*, 11928−11938.
(38) Chu, T.; Vyboishchikov, S. F.; Gabidullin, B.; Nikonov, G. I. Oxidative Cleavage of C═S and P = S Bonds at an All Center: Preparation of Terminally Bound Aluminum Sulfides. *Angew. Chem., Int. Ed.* **2016**, *55*, 13306−13311.
(39) Ballmann, J.; Yeo, A.; MacKay, B. A.; van Rijt, S.; Patrick, B. O.; Fryzuk, M. D. Complete disassembly of carbon disulfide by a ditantalum complex. *Chem. Commun.* **2009**, *46*, 8794−8796.
(40) Kalläne, S. I.; Braun, T.; Teltewskoi, M.; Braun, B.; Herrmann, R.; Laubenstein, R. Remarkable reactivity of a rhodium (i) boryl complex towards CO_2 and CS_2: isolation of a carbido complex. *Chem. Commun.* **2015**, *51*, 14613−14616.
(41) Johnson, A. R.; Davis, W. M.; Cummins, C. C.; Serron, S.; Nolan, S. P.; Musaev, D. G.; Morokuma, K. Four-Coordinate Molybdenum Chalcogenide Complexes Relevant to Nitrous Oxide N−N Bond Cleavage by Three-Coordinate Molybdenum(III): Synthesis, Characterization, Reactivity, and Thermochemistry. *J. Am. Chem. Soc.* **1998**, *120*, 2071−2085.
(42) Myers, A. W.; Jones, W. D.; McClements, S. M. Regiochemical Selectivity in the Carbon- Sulfur Bond Cleavage of 2-Methylbenzothiophene: Synthesis, Characterization, and Mechanistic Study of Reversible Insertion into a C-S Bond. *J. Am. Chem. Soc.* **1995**, *117*, 11704−11709.
(43) Bradley, C. A.; Veiros, L. F.; Chirik, P. J. C−O and C−S Bond Cleavage in Chelating Diethers and Thioethers Promoted by η^9,η^5-Bis(indenyl)zirconium Sandwich Complexes: A Combined Experimental and Computational Study. *Organometallics* **2007**, *26*, 3191−3200.
(44) McDonough, J. E.; Mendiratta, A.; Curley, J. J.; Fortman, G. C.; Fantasia, S.; Cummins, C. C.; Rybak-Akimova, E. V.; Nolan, S. P.; Hoff, C. D. Thermodynamic, Kinetic, and Computational Study of Heavier Chalcogen (S, Se, and Te) Terminal Multiple Bonds to Molybdenum, Carbon, and Phosphorus. *Inorg. Chem.* **2008**, *47*, 2133−2141.
(45) Atesin, T. A.; Kundu, S.; Skugrud, K.; Lai, K. A.; Swartz, B. D.; Li, T.; Brennessel, W. W.; Jones, W. D. Predicting Selectivity in Oxidative Addition of C−S Bonds of Substituted Thiophenes to a Platinum(0) Fragment: An Experimental and Theoretical Study. *Organometallics* **2011**, *30*, 4578−4588.
(46) Cardoso, D. V. V.; Cunha, L. A.; Spada, R. F. K.; Petty, C. A.; Ferrao, L. F. A.; Roberto-Neto, O.; Machado, F. B. C. Thermochemical and Kinetics of CH_3SH + H Reactions: The Sensitivity of Coupling the Low and High-Level Methodologies. *J. Phys. Chem. A* **2017**, *121*, 419−428.
(47) Jiang, X. F.; Huang, H.; Chai, Y. F.; Lohr, T. L.; Yu, S. Y.; Lai, W.; Pan, Y. J.; Delferro, M.; Marks, T. J. Hydrolytic cleavage of both CS_2 carbon-sulfur bonds by multinuclear Pd(II) complexes at room temperature. *Nat. Chem.* **2017**, *9*, 188−193.
(48) Yu, S.-Y.; Jiao, Q.; Li, S.-H.; Huang, H.-P.; Li, Y.-Z.; Pan, Y.-J.; Sei, Y.; Yamaguchi, K. Self-Assembly of Tripyrazolate-Linked Macrotricyclic $M_{12}L_4$ Cages with Dimetallic Clips. *Org. Lett.* **2007**, *9*, 1379−1382.
(49) Qin, L.; Yao, L.-Y.; Yu, S.-Y. Self-Assembly of $[M_8L_4]$ and $[M_4L_2]$ Fluorescent Metallomacrocycles with Carbazole-Based Dipyrazole Ligands. *Inorg. Chem.* **2012**, *51*, 2443−2453.
(50) Petrowsky, M.; Frech, R. Temperature Dependence of Ion Transport: The Compensated Arrhenius Equation. *J. Phys. Chem. B* **2009**, *113*, 5996−6000.
(51) Rocchigiani, L.; Ciancaleoni, G.; Zuccaccia, C.; Macchioni, A. Low-Temperature Kinetic NMR Studies on the Insertion of a Single Olefin Molecule into a Zr-C Bond: Assessing the Counterion−Solvent Interplay*. *Angew. Chem.* **2011**, *123*, 11956−11959.
(52) von Kugelgen, S.; Sifri, R.; Bellone, D.; Fischer, F. R. Regioselective Carbyne Transfer to Ring-Opening Alkyne Metathesis Initiators Gives Access to Telechelic Polymers. *J. Am. Chem. Soc.* **2017**, *139*, 7577−7585.
(53) Mloston, G.; Grzelak, P.; Hamera-Faldyga, R.; Jasinski, M.; Pipiak, P.; Urbaniak, K.; Albrecht, L.; Hejmanowska, J.; Heimgartner, H. Aryl, hetaryl, and ferrocenyl thioketones as versatile building blocks for exploration in the organic chemistry of sulfur. *Phosphorus, Sulfur Silicon Relat. Elem.* **2017**, *192*, 204−211.

DOI: 10.1021/acs.inorgchem.8b01275
Inorg. Chem. XXXX, XXX, XXX−XXX

(54) Gnanambal, K. M. E.; Patterson, J.; Patterson, E. J. K. Isolation of a Novel Antibacterial Phenyl Thioketone from the Seagrass, Cymodocea serrulate. *Phytother. Res.* **2015**, *29*, 554−560.
(55) Tulevski, G. S.; Miao, Q.; Afzali, A.; Graham, T. O.; Kagan, C. R.; Nuckolls, C. Chemical Complementarity in the Contacts for Nanoscale Organic Field-Effect Transistors. *J. Am. Chem. Soc.* **2006**, *128*, 1788−1789.

DOI: 10.1021/acs.inorgchem.8b01275
Inorg. Chem. XXXX, XXX, XXX−XXX